Quantification of Chemical-shift Apparent Diffusion Coefficients (ADC) of Fat and Water Signals Using Interleaved EPI based IDEAL Method and Multiplexed Parallel Image Reconstruction: *Application to studies of parotid glands*

Hing-Chiu Chang[1], Chun-Jung Juan[2], Hsiao-Wen Chung[3], Shayan Guhaniyogi[1], and Nan-Kuei Chen[1]

[1]*Brain Imaging and Analysis Center, Duke University Medical Center, Durham, North Carolina, United States,* [2]*Department of Radiology, Tri-Service General Hospital, Taipei, Taiwan,* [3]*Graduate Institute of Biomedical Electronics and Bioinformatics, National Taiwan University, Taipei, Taiwan*

Target Audience: Researchers and clinicians who are interested in chemical-shift ADC mapping of fat and water signals

Purpose: Quantification of chemical-shift apparent diffusion coefficients (ADC) of fat and water is very important for studies of many physiological systems such as liver and parotid glands. Although the ADC mapping of parotid glands can be performed with DW-PROPLELLER-FSE imaging with significantly reduced susceptibility artifact as compared with DW-EPI [1], the accuracy of ADC quantification may be reduced by residual fat signals from incomplete fat saturation [2]. The iterative decomposition with echo asymmetry and least squares (IDEAL) technique [3], which has been successfully applied to fat content quantification of the parotid glands in a recent report [4]. However, to our knowledge, the IDEAL based fat and water separation has not yet been applied to chemical-shift ADC mapping of parotid glands, because of several major technical challenges. First, the original IDEAL framework, designed for gradient-echo imaging based scans, is not compatible with EPI data in which the chemical-shift effect results in significant pixel displacement; second, because of the significant susceptibility field gradients near the parotid glands, the EPI-based ADC mapping is usually significantly distorted. To address these technical challenges to enable chemical-shift ADC mapping, here we first evaluate the IDEAL framework in the presence of large chemical-shift effect using both original and our modified frameworks. Second, we report a novel procedure that integrates 1) interleaved EPI sequence with reduced geometric distortion, and 2) aliasing artifact removal with multiplexed sensitivity encoding (MUSE) [5]. Our integrated technique reliably enables quantification of chemical-shifting ADC mapping of parotid glands, which cannot be achieved with conventional protocols.

Methods: First, our multi-shot interleaved DW-EPI pulse sequence is consisted of two parts: 1) image data acquisition with IDEAL-based echo shift (Fig.1a) and 2) parallel navigator echo (Fig.1b). Note that no RF based fat saturation is used our method. The shot-to-shot phase inconsistencies can be measured from navigator echoes, and the information can be used to eliminate motion-induced aliasing artifacts in interleaved EPI based DWI through the recently developed MUSE algorithm [5]. Next, we have modified the IDEAL framework to take the chemical-shift induced pixel displacement, which is unique to EPI data, into consideration. Specifically, the original signal IDEAL model was modified to $S(x,y,TE) = \left(W(x,y)e^{i\delta(x,y)TE'} + F(x,y-\Delta)e^{i\theta_{fat}TE}e^{i\delta(x,y-\Delta)TE'}\right)$, with W and F representing water and fat signals, δ being the field inhomogeneity term, and Δ being the chemical shift (in pixels) along the phase-encoding direction. This modified model shows that the signal in a certain voxel is the combination of local water signal and remote fat signal due to the field inhomogeneity induced chemical-shift artifact. Since there are generally four unknowns in this modified model (water, fat, and two local field inhomogeneity terms), we implemented a procedure to initiate the IDEAL processing in voxels with a only single inhomogeneity term, followed by full IDEAL processing for other voxels. We conducted a simulation study, to compare the original and the new EPI-compatible IDEAL reconstruction of simulated chemical-shift EPI data (with IDEAL TE shift by -0.2, 0.6, and 1.4ms; 30% fat-fraction; EPI chemical-shift artifact by 20 pixels; background field ranges: -150Hz to +150Hz). The chemical-shift interleaved DWI data were acquired from a healthy volunteer using a 4-shot interleaved diffusion-weighted EPI sequence (Fig.1) on a 3.0T MRI scanner (GE MR750, Waukesha, WI) using an 8-channel coil. Imaging parameters included: effective TEs=67ms with IDEAL shifting by -0.2, 0.6 and 1.4ms, TR=4000ms, ESP=0.7ms, FOV=24cm, matrix size=128x128, and b=800 s/mm^2. The EPI chemical-shift artifact (9.86 pixels) was corrected after fat-water separation.

Results: As compared with the input of our EPI simulation (Fig 2a), the water, fat and field inhomogeneity maps derived from the original IDEAL framework are negatively affected by the EPI chemical shift artifacts in the presence of large frequency offset such as -150Hz (see arrows in Fig 2b). Using our EPI-compatible IDEAL framework that takes the chemical-shift pixel displacement into consideration, the water, fat and inhomogeneities can be properly quantified, as shown in Fig 2c. Figure 3 further shows the dependence of water content quantification error (see color-bar) on field inhomogeneity (vertical axis) and water fraction (horizontal axis), which shows that the quantification error is less than 5% when the frequency offset is within -60Hz and 130Hz. The MUSE-produced human EPI (with TE shifted by -0.2ms) corresponding to b=0 (Fig.4a) and b=800 s/mm^2 (Fig.4b), and water and fat maps generated by the IDEAL framework are shown in Figure 4. The ADC maps calculated from water signals only, and both water and fat signals are shown in Figure 5.

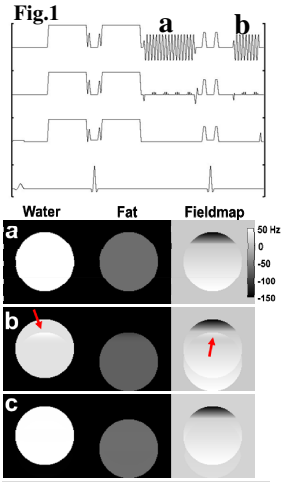

Fig.2 (a) The input of simulation. (b) The water, fat, and field inhomogeneity maps derived from the original IDEAL that is not compatible with EPI data. (c) The water, fat, and field maps derived from our EPI-compatible IDEAL framework are free from artifacts related chemical- shift EPI pixel displacement in the presence of large frequency offset due to field inhomogeneities.

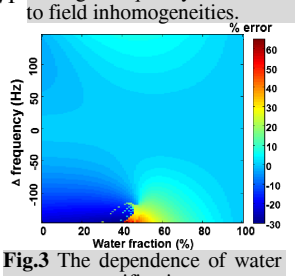

Fig.3 The dependence of water content quantification errors on field inhomogeneities and water fraction.

Discussion & Conclusion: Because of strong local susceptibility field gradients, interleaved EPI with inherently reduced geometric distortions is superior to single-shot EPI for ADC mapping of parotid glands. Since the interleaved DWI is susceptible to undesirable motion-induced aliasing artifact, we needed to use the recently developed MUSE method to effectively remove artifacts and produce high-quality images, as the input of subsequent IDEAL data processing. The original IDEAL framework is not compatible with EPI data affected by chemical-shift induced pixel displacement in the presence of large field inhomogeneity difference between local water and remote fat signals, as shown in Fig 2b. The simulation on the water content quantification error from IDEAL framework (Fig.3) shows a wide acceptable range of field inhomogeneity. Moreover, as compared with single-shot EPI, 4-shot interleaved EPI acquisition has a larger bandwidth per pixel value and thus can better tolerate field inhomogeneities, resulting in ignorable fat-water separation error even using the original IDEAL framework. In conclusion, using the integration of interleaved DWI and MUSE reconstruction, we have successfully acquired chemical-shift ADC maps of parotid glands. We expect that the developed technique should also play an important role for chemical-shift ADC mapping of liver and other body organs as well.

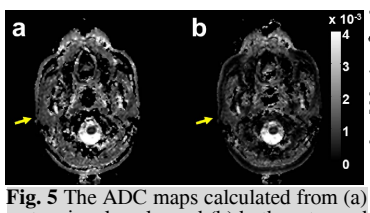

Fig. 5 The ADC maps calculated from (a) water signals only, and (b) both water and fat signals.

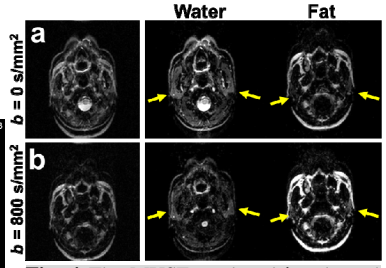

Fig. 4 The MUSE-produced interleaved EPI data (with TE shifted by -0.2ms) corresponding to (a) b=0 s/mm2 and (b) b=800 s/mm2, and water and fat maps derived from the IDEAL framework.

References: [1] Juan CJ, et al., Radiology;253(1):144, 2009. [2] Chiu HC, et al., 18th ISMRM, #4308. [3] Reeder SB, et al., JMRI;(25):644, 2007. [4] Chang HC, et al., Radiology;267(3):918, 2013. [5.] Chen NK, et al., Neuroimage;(72):41-47, 2013.